Isı Bilimi ve Tekniği Dergisi, 42, 2, 269-280, 2022
J. of Thermal Science and Technology
©2022 TIBTD Printed in Turkey
ISSN 1300-3615
https://doi.org/10.47480/isibted.1203793

ANALYSIS OF HEAT TRANSFER ENHANCEMENT IN TUBES WITH CAPSULE DIMPLED SURFACES AND Al_2O_3-WATER NANOFLUID

Ekin ÖZGİRGİN YAPICI[*], Mahmoud Awni A. Haj IBRAHIM[**] and Haşmet TÜRKOĞLU[***]
Çankaya University, Department of Mechanical Engineering, Etimesgut, Ankara
[*]ekinozgirgin@cankaya.edu.tr, ORCID: 0000-0002-7550-5949
[**]mahmoud.awni96@gmail.com, ORCID: 0000-0002-7932-9583
[***]hasmet@cankaya.edu.tr, ORCID: 0000-0002-1941-986X

(Geliş Tarihi: 09.08.2022, Kabul Tarihi: 24.10.2022)

Abstract: This study aims to numerically investigate and evaluate the enhancement of heat transfer by new capsule dimples on tube surfaces for flow of water and Al_2O_3-water nanofluid with different concentrations, under uniform surface heat flux. The originality of this work lies in combining two passive heat transfer enhancement methods such as geometrical improvements and nanofluids together. Capsule dimples with different depths were considered. Al_2O_3-water nanofluid was modeled as a single-phase flow based on the mixture properties. The effects of dimple depth and nanoparticle concentrations on Nusselt number, friction factor and performance evaluation criteria (PEC) were studied. Numerical computations were performed using ANSYS Fluent commercial software for 2000-14000 Reynolds number range. It was found that when laminar, transient and fully developed turbulent flow cases are considered, increase in the dimple depth increases the Nusselt number and friction factor for both pure water and Al_2O_3-water nanofluids cases. Also, the friction factor increases as dimple depth increases. Results show that increase in PEC is more pronounced in the laminar region than in the transition region, it starts to decrease for turbulent flows. For nanofluid, PEC values are considerably higher than pure water cases. The variation of PEC for capsule dimpled tubes are dependent on flow regimes and dimple depths. Increasing the nano particle volume concentration and dimple depth in laminar flows increase the PEC significantly.
Keywords: Heat transfer enhancement, nanofluid, capsule dimples, computational analysis

BORU YÜZEYİNDEKİ KAPSÜL TİPİ KABARTMANIN VE Al_2O_3-SU NANOAKIŞKANIN ISI TRANSFERİNE ETKİSİNİN SAYISAL ANALİZİ

Özet: Bu çalışmanın amacı, duvar yüzeyinden düzenli ısı akısı uygulanan boru içi akışlarda geometrik modifikasyon yapılarak elde edilecek ısı transferi iyileştirmesinin numerik olarak incelenmesidir. Geometrik modifikasyon olarak kapsül tipi kabartmalar kullanılmış, akışkan olarak ise su ve Al2O3-su nano-akışkan kullanılmıştır. Isı transferi iyileştirmesi için hem geometrik modifikasyon yapılmış olması hem de bununla birlikte farklı yüzdelerde nano-akışkan kullanılmış olması çalışmayı benzerlerinden farklı bir noktaya taşıyabilmektedir. Kapsül tipi kabartmalar borunun iç yüzeyine farklı derinliklerde uygulanmıştır. Al2O3-su nano-akışkan 1%, 2% ve 3% konsantrasyonlarında tek fazlı akış olarak modellenmiş ve uygulanmıştır. Kabartmaların derinliğinin ve nono-akışkanın farklı konsantrasyonlarda uygulamalarının Nusselt sayısı, Sürtünme katsayısı ve Performans Değerlendirme Kriteri (PEC) üzerindeki etkileri çalışılmıştır. Sayısal analizler ANSYS Fluent kullanılarak 2000-14000 Reynolds Sayısı aralığında gerçekleştirilmiştir. Sonuçlar incelendiğinde, tüm akışkanlar için, laminer akış, geçiş akışı ve tamamen gelişmiş türbülanslı akış durumunda kabartma derinliği arttıkça Nusselt Sayısı ve aynı zamanda da sürtünme katsayısının arttığı görülmüştür. Laminer rejimde PEC daki artış etkisi türbülans rejimine göre oldukça fazladır. Performans Değerlendirme Kriterinin değişimi akış rejimine ve kabartma derinliğine oldukça bağlıdır. Genel olarak, laminer akışta nano-akışkan konsantrasyonu ve kabartma derinliği arttıkça Performans Değerlendirme Kriterinin önemli ölçüde arttığı görülmüştür.
Anahtar Kelimeler: Isı transferi iyileştirmesi, nano-akışkan, kapsül tipi kabartma, sayısal analiz

INTRODUCTION

Heat transfer in tubes is a field of interest for many researchers due to its usability and accessibility in many engineering applications, such as heat exchangers, which are widely used in refrigeration, air conditioning, space heating, power generation, chemical processing for cooling or heating purposes, district heating systems,

renewable energy systems, geothermal water distribution systems, solar collectors, etc.

In the variety of these applications, main challenge is to increase the heat transfer performance of the systems per unit area or volume regarding the limits of sizing to achieve this goal. This challenge offers an opportunity for improvement to develop methods to make heat transfer equipment more compact and achieve a high heat transfer rate using less pumping power to minimize the energy and material costs. For this, the most effective parameter is the heat transfer coefficients on the hot and cold fluid sides, and the heat transfer coefficient can be increased by one or more active or passive methods.

Methods that improve heat transfer by giving additional energy are called active methods such as surface vibration and flow vibration, electrostatic fields, and mechanical aids. Methods that improve heat transfer rate without additional energy requirement are called the passive method which include surface geometrical modifications to increase the heat transfer surface area or using additives in the working fluid, such as nanoparticles. Passive methods are more advantageous than active methods since they do not require external energy and are easier to apply. In the scope of this study, two passive methods have been employed for heat transfer enhancement.

Most common passive methods of geometrical modifications found in the literature include louvered strips (Eiamsa-Ard et al.,2008), twisted tapes (Tabatabaeikia et al., 2014), helical screw inserts (Pathipakka et al., 2010), wire coil insert (Chandrasekar et al., 2013) and dimples on the tube surface Li et al. (2015). These are used to increase the turbulent flow characteristics through the tube and thus enhance the heat transfer coefficient. One of the most applicable and advantageous passive methods is using three-dimensional dimples along the heat transfer surface. The main reason of heat transfer enhancement along the dimple surface is that thermal boundary layer formation is disturbed and hence, Nusselt number and heat transfer coefficient increases. (Cheraghi et al., 2019)

While increasing the heat transfer coefficient, geometrical modifications may also cause increase in the friction which is generally not desired. As result of increase in the friction, the pressure drop and necessary pump/compressor work increases. Thus the proper design and application of geometrical modifications, including the dimples, is crucial. For this reason, a dimensionless performance evaluation criterion (PEC) is used to assess the thermal-hydraulic performance of heat transfer enhancement techniques. (Li et al., 2016).

Flow regime is found to have a significant effect on the heat transfer performance. Enhancement of heat transfer using dimpled tubes has been studied for different Reynolds numbers in the literature.

Cheraghi et al., (2020) conducted a numerical study on a new configuration of deep dimpled tube under constant heat flux to evaluate the effects of dimple pitch, dimple diameter and dimple depth on the heat transfer and flow field for considering Reynolds numbers of 500, 1,000 and 2,000. The study showed that decreasing the distance between dimples while increasing the dimple depth and diameter would result increase in the Nusselt number and friction factor. A sudden growth in the friction factor is observed due to the formation of vortexes behind each dimple, causing a larger pressure drop than that of plain tubes. According to the performance evaluation criteria, the higher enhancement for the deep dimpled tubes can be achieved by increasing the dimple diameter, pitch and Reynolds number and reducing the dimple depth.

On the transitional ($2000<Re<4000$) and the moderate ($4000<Re<10000$) ranges of Reynolds numbers, (Vicente et al., 2002) experimentally studied flow and heat transfer in helically dimpled tubes by using water and ethylene glycol and ten different configurations of tubes with various depths and pitches of dimples. The results showed that as the depth of dimples increased, the heat transfer performance of the tube improved.

On higher Reynolds numbers, (turbulent flow $Re>10000$), (Kumar et al.,2017) experimentally and numerically investigated the effects of dimples on the heat transfer and hydrodynamics performance of dimpled tubes for Reynolds numbers between 4,000 and 28,000 and using air as the working fluid. The study showed that the highest Reynolds numbers yielded the highest Nu and lowest friction factor as expected. On the other hand, increasing the stream and span-wise direction to a certain extent would positively affect heat transfer enhancement, and both thermal and hydraulic performance would increase if the stream and span-wise directions decrease. The author revealed that the optimum thermal and hydraulic performance is reached when stream and span-wise direction had the value of 15 times the dimple diameter.

Shape, size, depth, and pitch of the dimples are important properties that affect heat transfer performance in such flows. Ming et al. (2016) numerically studied the effects of geometrical parameters on heat transfer and pressure loss inside a dimpled tube. The results showed that the reduction in the pitch of dimples and increase in the depth contributed to the heat transfer enhancement. However, these variations increased the pressure loss.

Wang et al. (2010) experimentally investigated the heat transfer enhancement and friction factor of different shape dimpled tubes. Experimental data showed that tubes with ellipsoidal dimples simultaneously had higher Nusselt number and lower friction factor than the tubes with spherical dimples. Also, ellipsoidal dimples

roughness accelerated the transition to critical Reynolds number down to less than 1000.

Chen et al. (2001) experimentally studied six different dimpled tubes with different dimple parameters, ratio of depth to tube diameter, depth to pitch ratio and number of dimples on the tube surface. The Reynolds numbers taken in this experiment had ranged from 7,500 to 52,000. It was found that the enhancement in heat transfer reached 137% compared to standard plain tubes and the performance criteria showed values from 0.93 to 1.16 in which the dimpled tube with values above unity were considered to succeed in the performance enhancement.

Another important heat transfer enhancement method employs nanoparticles suspended in water solutions, called nanofluids to improve the thermo-physical properties of the working fluid. Combining this technique with surface alterations makes further enhancement of heat transfer characteristics. Nanofluids have proven to affect heat transfer positively, and the use of nanofluids in many research applications has been of interest to researchers, especially in the heat transfer and fluid dynamics communities due to advantages in improving heat transfer rate.

Because metals have higher thermal conductivity than nonmetals, metallic or metal oxide nanofluids have been chosen for heat transfer fluid. Xuan and Li (2000) achieved a remarkable heat transfer enhancement of 39% using 2% volume fraction of Cu nanoparticles dispersed in water. Briclot et al. (2020) have also accomplished a 40% increment in Nusselt number using Al_2O_3water nanofluid with a volume fraction of 6.8% in their study intended for liquid cooling of electronic components. (Firoozi et al. 2020)

Khedkar et al. (2014) experimentally investigated the effect of different nanoparticle concentrations of a TiO_2-water base nanofluid on the heat transfer performance in a concentric tube heat exchanger; hence the use of nanofluid was for cooling purposes in which the inner tube was for the nanofluid, and the outer tube was for water as a hot fluid. The coolant working range of this experiment had Reynolds numbers ranging from 300 to 4,000. They investigated the effects of different nanoparticle concentrations (2% and 3%), and showed that increasing the Reynolds number resulted in a significant increase in heat transfer performance compared to pure water as a cooling fluid.

Ho et al. (2018) performed experimental investigations on a tube with circular cross-sections under constant heat flux for laminar flow with Reynolds numbers ranging from 120 to 2,000 using an Al_2O_3-water nanofluid as a working fluid. To evaluate the effects of the nanofluid subjected to variable operating temperatures on heat transfer characteristic and pressure differences, an additional numerical study was conducted. The results proved that using Al_2O_3 nanoparticles in a water based nanofluid for forced heat transfer applications would minimize the temperature difference between the mean fluid temperature and wall temperature that results a better heat transfer characteristic but increases the pressure drop.

In this study, heat transfer enhancement by new capsule dimpled tube surfaces is numerically investigated with pure water and Al_2O_3-water nanofluid for different geometrical properties of dimpled tubes and different concentrations of nanoparticles. Heat transfer enhancement regarding Nusselt number and heat transfer coefficient, and pressure drop regarding friction factor changes are investigated, and performance evaluation criteria is calculated and compared for different cases.

METHODOLOGY

In the present study, flow of pure water and Al_2O_3-water nanofluid in a dimpled tube with a constant surface heat flux was considered. Methodology followed is based on the mathematical modelling and numerical solution of the governing equations. ANSYS Fluent was used for the numerical simulations. Then, from the numerically obtained temperature and flow fields, the heat transfer coefficient and friction factor were calculated. Different cases were simulated and compared to evaluate the effects of the dimple geometrical parameters, Reynolds number and nano particle concentration on heat transfer coefficient and PEC.

Problem Geometry and Mathematical Formulation

The geometry of the flow domain considered in the study is shown in Fig. 1. As seen in the figure, heat transfer surface has capsule dimples, and the flow domain is extended with an undimpled inlet section. The tube cross section is circular. Fluid is flowing through the tube. A constant heat flux is applied through the outer surface.

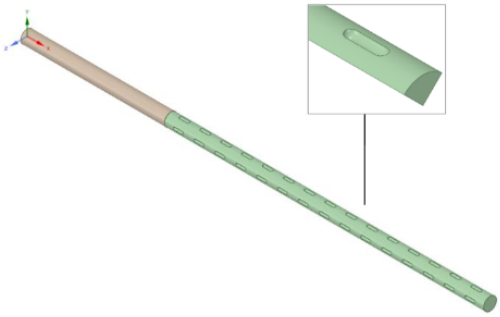

Figure 1. Capsule dimpled tube with undimpled entrance section and a periodic quarter sector used for the analysis.

As shown in Fig. 1, the tube consists of 200 mm undimpled entrance length and 440 mm dimpled region. The tube diameter is 18 mm and kept constant for all the simulations.

A sketch of the geometry of dimples is shown in Fig. 2. As seen in this figure, a dimple is characterized by depth (h), length (d), pitch (P) and length from center to center (w). In the present study, dimple depth is varied as all other dimple parameters are kept constant.

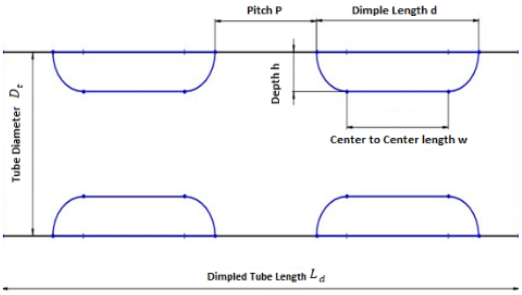

Figure 2 Schematics view of the dimple geometry and important dimple parameters.

Governing Equations

To derive the governing equations for the current physical problem, the equations of conservation of mass, Newton's Second Law, and the Law of Conservation of Energy should be formulated. For the derivation of the governing equations the following assumptions were made: Flow is three-dimensional, steady, viscous, incompressible, turbulent, body forces are negligible, working fluid properties are constant, and the fluid is Newtonian.

In addition, it is assumed that the nano particle distribution in the flow field is uniform, nanoparticles and the base fluid are in thermal equilibrium, and the velocities of the nanoparticles and base fluid are equal. The physical properties of the nanoparticle-water mixture are calculated using the correlations in the literature as given below.

Based on the above assumptions, Reynolds averaged governing equations can be written as below:

Continuity equation:

$$\frac{\partial \bar{u}}{\partial x}+\frac{\partial \bar{v}}{\partial y}+\frac{\partial \bar{w}}{\partial z}=0 \tag{1}$$

Where $\bar{u}$, $\bar{v}$ and $\bar{w}$ are the time-averaged velocity components in the x, y and z directions, respectively

Momentum equations:

x-direction:

$$\rho_{nf}\left(\bar{u}\frac{\partial \bar{u}}{\partial x}+\bar{v}\frac{\partial \bar{u}}{\partial y}+\bar{w}\frac{\partial \bar{u}}{\partial z}\right)=-\frac{\partial p}{\partial x}+\mu_{nf}\left(\frac{\partial^2 \bar{u}}{\partial x^2}+\frac{\partial^2 \bar{u}}{\partial y^2}+\frac{\partial^2 \bar{u}}{\partial z^2}\right)-\left(\frac{\partial \overline{u'^2}}{\partial x}+\frac{\partial \overline{u'v'}}{\partial y}+\frac{\partial \overline{u'w'}}{\partial z}\right) \tag{2}$$

y-direction:

$$\rho_{nf}\left(\bar{u}\frac{\partial \bar{v}}{\partial x}+\bar{v}\frac{\partial \bar{v}}{\partial y}+\bar{w}\frac{\partial \bar{v}}{\partial z}\right)=-\frac{\partial p}{\partial y}+\mu_{nf}\left(\frac{\partial^2 \bar{v}}{\partial x^2}+\frac{\partial^2 \bar{v}}{\partial y^2}+\frac{\partial^2 \bar{v}}{\partial z^2}\right)-\left(\frac{\partial \overline{v'u'}}{\partial x}+\frac{\partial \overline{v'^2}}{\partial y}+\frac{\partial \overline{v'w'}}{\partial z}\right) \tag{3}$$

z-direction:

$$\rho_{nf}\left(\bar{u}\frac{\partial \bar{w}}{\partial x}+\bar{v}\frac{\partial \bar{w}}{\partial y}+\bar{w}\frac{\partial \bar{w}}{\partial z}\right)=-\frac{\partial p}{\partial z}+\mu_{nf}\left(\frac{\partial^2 \bar{w}}{\partial x^2}+\frac{\partial^2 \bar{w}}{\partial y^2}+\frac{\partial^2 \bar{w}}{\partial z^2}\right)-\left(\frac{\partial \overline{w'u'}}{\partial x}+\frac{\partial \overline{w'v'}}{\partial y}+\frac{\partial \overline{w'^2}}{\partial z}\right) \tag{4}$$

In these equations, p, ρ_{nf} and μ_{nf} denote the pressure, effective density (mixture density) and effective viscosity (mixture viscosity) of the nanofluid, respectively.

Energy equation:

$$div\left(\rho_{nf}\bar{V}C_{p,nf}\bar{T}\right)=div\left(k_{nf}\,grad\,(\bar{T})-\rho_{nf}\overline{T'}C_{p,nf}\overline{V'}\right) \tag{5}$$

where, T is the temperature, k_{nf} is the effective thermal conductivity (mixture conductivity) and $C_{p,nf}$ is the effective specific heat (mixture specific heat) of the nanofluid.

Boundary conditions

Considering the physics of the problem described above, the boundary conditions can be expressed as follows:

- The velocity at the inlet is only in axial direction and uniform.
- Inlet temperature is uniform and constant (293 K).
- Uniform heat flux is applied along the surface of the tube (10,000 W/m^2).
- The exit gage pressure is zero.

Further explanations regarding boundary conditions are found in the following parts.

Properties of nanofluid

The properties of the nanofluid are calculated using the equations proposed by different researchers in the literature.

Calculation of nanofluid density is carried out using the correlation proposed by Cho and Pak (1998) as below:

$$\rho_{nf}=(1-\varphi)\rho_{bf}+\varphi\rho_{np} \tag{6}$$

where φ, *is* volume concentration of the nano particles, the subscripts *bf* and *np* refer to base fluid and nanoparticles, respectively.

The effective specific heat of the nanofluid $(C_p)_{nf}$ can be calculated based on the expression proposed by Xuan and Roetzel (2000):

$$(C_p)_{nf}=\frac{(1-\varphi)(\rho C_p)_{bf}+\varphi(\rho C_p)_{np}}{\rho_{nf}} \tag{7}$$

The Maxwell's model (1954) is used for evaluation of the thermal conductivity as shown below:

$$k_{nf} = \frac{k_{np}+2k_{bf}-2\varphi(k_{bf}-k_{np})}{k_{np}+2k_{bf}+\varphi(k_{bf}-k_{np})}k_{bf} \quad (8)$$

where k_{np}, k_{bf} and φ are the thermal conductivity of nanoparticles, thermal conductivity of the fluid and the volume concentration, respectively.

For the calculation of the effective viscosity, expression developed by Pak and Cho (1998) is used.

$$\mu_{nf} = \mu_{bf}(1 + 39.11\varphi_{np} + 533.9\varphi^2_{np}) \quad (9)$$

Important Flow Parameters

Reynolds number is one of the important parameters used to characterize fluid flows. For the problem under consideration, Reynolds number is defined in terms of mixture properties as:

$$\mathrm{Re} = \frac{\rho_{nf}\mathrm{UD_h}}{\mu_{nf}} \quad (10)$$

where ρ_{nf} is the nanofluid density, U the average velocity, D_h the hydrodynamic diameter (for circular tube D_h being the same as the tube diameter) and μ_{nf} is the dynamic viscosity of the nanofluid.

Nusselt number quantifies the convection heat transfer relative to conduction heat transfer within a fluid layer (Cengel, 2014). The average Nusselt number is defined as

$$\mathrm{Nu} = \frac{hD_h}{k_{nf}} \quad (11)$$

where h, k_{nf} and D_h are the average heat transfer coefficient, thermal conductivity of nanofluid and hydraulic diameter of the tube, respectively.

The average friction factor for the plain tube and capsule dimpled tube are calculated using the Darcy equation as (Cengel, 2014):

$$f = \frac{2D_h\Delta p}{\rho_{nf}LU^2} \quad (12)$$

To ensure that the flow is hydrodynamically fully developed before entering the dimpled tube, it is important to have the necessary entrance length. To meet this requirement, the tube is extended by a plain section at inlet end as seen in Fig. 1.

Heat Transfer Enhancement and Performance Evaluation Criteria

Contribution of the dimples to the heat transfer rate is determined by comparing the Nusselt number with the Nusselt number for non-dimpled plain cases. For the estimation of the enhancement, heat transfer enhancement ratio (ER), which is the ratio of the Nusselt number in an enhanced case (dimpled tube) to the Nusselt number in the plain tube case (plain tube) (Kukulka et al., 2013), i.e.

$$ER = \frac{\mathrm{Nu_d}}{\mathrm{Nu_p}} \quad (13)$$

Since the geometrical modification at the heat transfer surface may cause an increase in the pressure drop (friction coefficient), a performance criterion combining the Nusselt number and friction coefficient (pressure drop) is defined. This criterion is known as Performance evaluation criteria (PEC), and different expression are proposed. PEC is the ratio of heat transfer enhancement to the hydraulic losses. Expression used for PEC proposed by Gee and Webb (1980) is given as:

$$PEC = \frac{\frac{Nu_d}{Nu_p}}{\left(\frac{f_d}{f_p}\right)^{\frac{1}{3}}} \quad (14)$$

In this study the performance evaluation criterion (PEC) is used to estimate the performance of the different cases considered.

Turbulence Equations

In the current study, laminar, transient, and turbulent flows were considered. Literature review shows that for low Reynolds number flows (one considered in this study) the realizable k-ε model yields better predictions in near wall flows in comparison to other turbulence models (Alshehri et al., 2020). Hence, the realizable k-ε turbulence model was chosen for the numerical simulations.
For turbulent kinetic energy k, the transport equation is;

$$\frac{\partial(\rho k u_i)}{\partial x_i} = \frac{\partial}{\partial x_i}\left[\left(\mu + \frac{\mu_t}{\sigma_k}\right)\frac{\partial k}{\partial x_i}\right] + G_k - \rho\epsilon - Y_M \quad (15)$$

Where G_k, Y_M and σ_k represent the generation of turbulent kinetic energy due to the mean velocity gradient, the contribution of fluctuating dilatation in compressible turbulence to overall dissipation rate and a turbulent Prandtl number for k, respectively.

In addition, the transport equation for the turbulent kinetic energy dissipation rate (ϵ), is written as:

$$\frac{\partial(\rho\epsilon u_i)}{\partial x_i} = \frac{\partial}{\partial x_i}\left[\left(\mu + \frac{\mu_t}{\sigma_\epsilon}\right)\frac{\partial \epsilon}{\partial x_i}\right] + \rho C_1 S\epsilon - \rho C_2 \frac{\epsilon^2}{k+\sqrt{\nu\epsilon}} \quad (16)$$

where;

$$C_1 = \max\left[0.43, \frac{\eta}{\eta+5}\right], \eta = \frac{k}{\epsilon}\sqrt{2S_{ij}S_{ij}} \quad (17)$$

The constants are: $C_2 = 1.9$, $\sigma_k = 1.0$ and $\sigma_\epsilon = 1.2$.

The eddy viscosity μ_t is calculated as

$$\mu_t = \rho C_\eta \frac{k^2}{\epsilon} \quad (18)$$

C_η is calculated as

$$C_\eta = \frac{1}{A_0 + A_s\frac{kU^*}{\epsilon}} \quad (19)$$

where

$$U^* = \sqrt{S_{ij}S_{ij} + \widetilde{\Omega}_{ij}\widetilde{\Omega}_{ij}}, A_0 = 4.04, A_s = \sqrt{6}\cos\emptyset \quad (20)$$

$$\emptyset = 3\cos^{-1}\sqrt{6}W \text{ and } W = \frac{S_{ij}S_{ik}S_{ki}}{\tilde{S}^3} \quad (21)$$

and

$$\tilde{S} = \sqrt{S_{ij}S_{ij}}, \quad \widetilde{\Omega}_{ij} = 0.5\left(\frac{\partial u_j}{\partial x_i} + \frac{\partial u_i}{\partial x_j}\right) \quad (22)$$

NUMERICAL SOLUTION

ANSYS Fluent software is utilized to solve the nonlinear governing equations presented in the previous part for the described physical problem of steady, incompressible, turbulent flow and heat transfer in a capsule dimpled tube with water and nanofluid as the working fluids.

The pressure and velocity coupling the Semi-Implicit Method for Pressure Linked Equations (SIMPLE) algorithm is used. Momentum and energy equations are discretized by the second order upwind scheme. For the convergence criteria, the residuals for all the variables are set to 10^{-6}.

Mesh Generation and Mesh Independence Study

To ensure the reliability and compatibility of the numerical results, a good computational mesh should be generated. As seen in Fig. 3, a quarter sector of the pipe enclosing one row of the dimples was considered as the computational field. Due to the 3-dimensional capsule geometry, a 3-dimensional mesh is formed. (For the simulations in plain pipes a 2-D mesh system is used.) To resolve the sublayer regions developed near the tube wall, a fine mesh structure usually with $y^+ \cong 1$ is implemented. The tetrahedral mesh structure was used, and it was produced using ANSYS meshing tool.

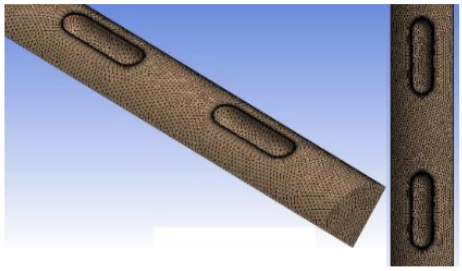

Figure 3. Mesh structure of capsule dimpled tube.

To verify the validity of the simulation results and keeping the computational costs as low as possible, a mesh independence study was conducted. For the mesh independence study, case with Reynolds numbers 14,000 is considered and computations were repeated with different mesh sizes. To determine the optimum mesh size, Nusselt numbers obtained with different mesh sizes for different dimple depths were compared. The average Nusselt numbers calculated from the numerical results with different meshes are shown in Fig. 4 and Fig. 5 for plain and dimpled tubes, respectively.

Analysis of Fig. 4 shows that a mesh 700,000 with nodes yields mesh independent results for plain pipe flows considered. Also, from Fig. 5 conclude that a mesh of 3.0 million nodes is good for mesh independent results for different dimple depths considered. Hence, for all the plain tube simulations and dimpled tube cases, mesh size of 700,000 and 3.0 million was used, respectively.

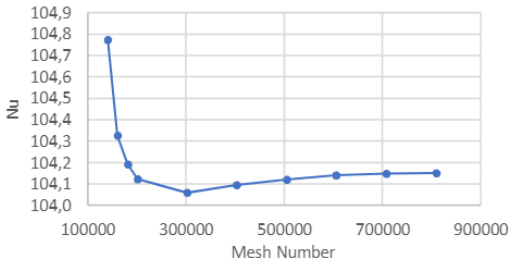

Figure 4. Variation of Nusselt number obtained with mesh number for the plain tube.

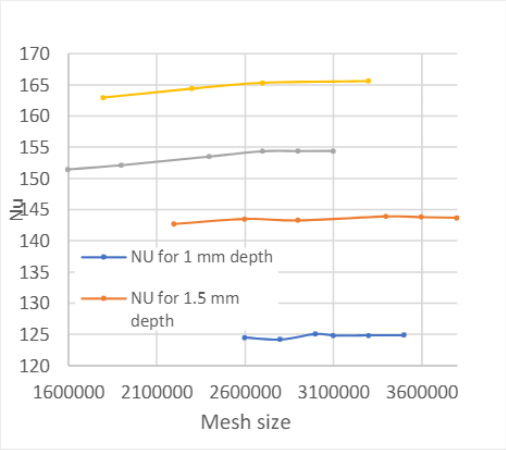

Figure 5. Variation of Nusselt numbers obtained with mesh sizes for dimple depths of 1.0, 1.5, 2.0 and 2.5 mm.

Comparison of Turbulence Models

To assess the suitability of the turbulence model used, a sequential study was conducted for flows with different Reynolds numbers using different turbulence models (realizable k-ε, standard k-ε with enhanced wall treatment for the near wall flow and the SST k-ω). The Nusselt numbers and friction factors are obtained with different models and compared with the Petukhov correlation given below (Cengel, 2014):

$$Nu = \frac{\left(\frac{f}{8}\right)(Re-1000)Pr}{1+12.7\left(\frac{f}{8}\right)^{0.5}\left(Pr^{\frac{2}{3}}-1\right)} \quad (23)$$

This correlation is valid for the ranges of $3{,}000 < Re < 5\times10^6$ and $0.5 \leq Pr \leq 2{,}000$.

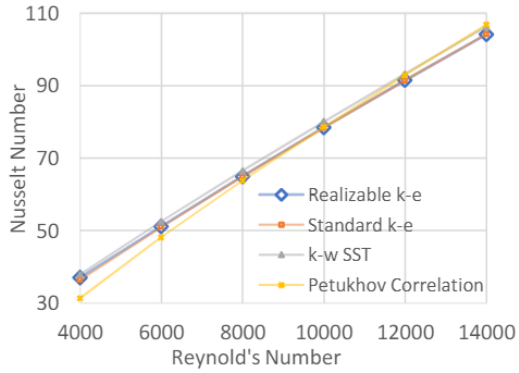

Figure 6. Comparison of Nusselt Numbers obtained using different turbulence models with the Petukhov correlation

As seen in Fig. 6, Nusselt numbers for the realizable k-ε model has a better approach than the other models for all Reynolds numbers being considered. Based on that, the realizable k-ε turbulence model is selected.

Validation of Numerical Results

To validate the numerical method and computer program used in the present study, a verification study was carried out considering the flow of water in the plain and dimpled tubes separately.

Numerical computations were performed for flows with different Reynolds numbers. The Nusselt numbers calculated from the numerical results and Nusselt numbers calculated from Petukhov correlation were calculated and compared in Fig. 7. As seen in Fig. 7, the results show a good agreement. For the case of a fully developed laminar flow, Nusselt number was calculated as 4.29, which is excepted when compared with the literature (Cengel, 2014).

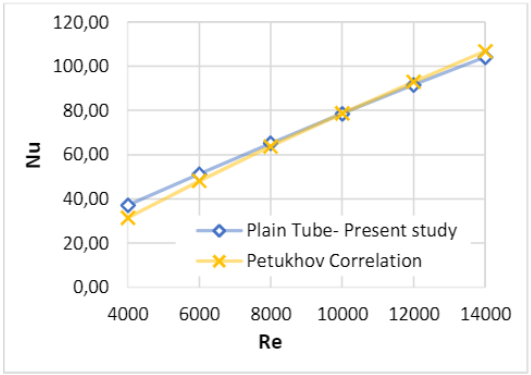

Figure 7. Comparison of numerically calculated Nusselt numbers with Petukhov correlation in plain tube.

The friction factor calculated from the numerical results in the plain tube also shows good agreement with the Petukhov correlation given below, with an average value of 0.03 and the errors fall within the acceptable range.

$$f = (0.790\ ln Re - 1.64)^{-2} \quad (24)$$

Validity range of this expression is $3000 < Re < 5\times10^6$.

To demonstrate the validity of the numerical results in the dimpled tubes, a verification study was carried out based on the study by Sabir et al. (2020) in ellipsoidal dimpled tube. The tube used in the study has a diameter of 17.3 mm, dimple diameter and depth are 3.9 mm and 1.17 mm, respectively with a pitch of 10 mm. A constant heat flux of 10,000 W/m^2 was applied.

The Nusselt numbers are compared in Fig 8. Maximum difference in the Nusselt numbers is calculated about 10%. The average friction factor is calculated as 0.06 and compared with the results given by Sabir et al. (2020) a 15% difference is observed. These differences are considered in the acceptable ranges.

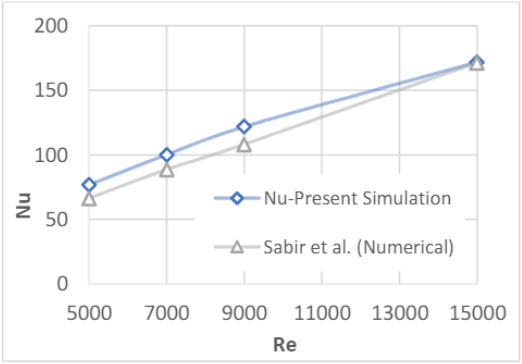

Figure 8. Comparison of numerically calculated Nusselt numbers with study of Sabir et al. (2020) for dimpled tubes.

RESULTS AND DISCUSSIONS

The objective of the study is to investigate the heat transfer enhancement for a tube flow using dimpled tube surface and nanofluid. For this purpose, numerical simulations were performed in plain and dimpled tubes. To investigate the effects of dimple depth on the heat transfer rate, the computations were performed with dimple depths of 1, 1.5, 2 and 2.5 mm for pure water flow and nanofluid flow with nanoparticle volumetric concentrations of 1%, 2% and 3%. The values of geometrical parameters of the tube and dimples are given in Table 1. The computations were performed for Reynolds numbers 2,000, 4,000, 6,000, 8,000, 10,000, 12,000 and 14,000.

Table 1. Values of tube and of dimple geometric parameters.

Tube Diameter D_t	18 mm
Length of dimpled section L_d	440 mm
Dimple length d	12/13/14/15 mm
Pitch P	15 mm
Dimple Depth h	1/1.5/2/2.5 mm
Center to center length w	10 mm
Entrance Length	12,000 mm (Laminar) 200 mm (Turbulent)

As the nanofluid, water-Al_2O_3 mixture is used. Thermophysical properties of the Al_2O_3-water nanofluid are calculated using the expressions given in Section 2 and given in the Table 2 for different volume concentrations (Minea, 2017).

Table 2. Thermophysical properties of Al_2O_3-water nanofluid for different nanoparticle volume concentrations

Volume Concentration (%)	ρ (kg/m^3)	μ (Pa.s)	c_p (J/kgK)	k (W/mK)
1	1,026.2	0.001444	4,048.8	0.63
2	1,056	0.001996	3,924.2	0.649
3	1,085.7	0.002654	3,806.3	0.667

The simulations were performed first for plain tube cases using pure water and nanofluid as working fluid. Then for dimpled tubes again for pure water and nanofluid as working fluid. The effects of Reynolds number, dimple depth and nanoparticle volumetric concentration on Nusselt number and friction factor are calculated. To characterize the heat transfer enhancement, the performance evaluation criteria (PEC) is also calculated for all the cases considered. The results are presented as graphs and analyzed below.

Effects of Capsule Dimples

Fully developed flow enters the dimpled tubes. Due to the dimples on the surface, considerable changes take place in the velocity and temperature fields, especially near the tube wall. Velocity increases and drops form because of the change in the flow cross sectional area due to the dimples.

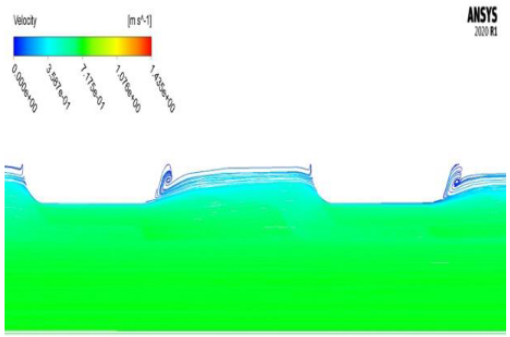

Figure 9. Velocity contours at a section of dimpled pipe for the flow of pure water flow with Re=10000 and dimple depth of 2 mm.

For the flow of pure water with Re=10000 and dimple depth of 2 mm, velocity contours for the dimples at the middle of the pipe on z direction along the flow are given in Fig. 9. As seen in Fig. 9, over the dimples, boundary layer thickness decreases while some recirculation forms between the dimples at downstream face of the dimples.

From the temperature field calculated, the average heat transfer coefficients and then average Nusselt numbers were calculated for the flow of pure water at different Reynolds numbers in tubes with different dimple heights. These Nusselt number results are shown in Fig. 10.

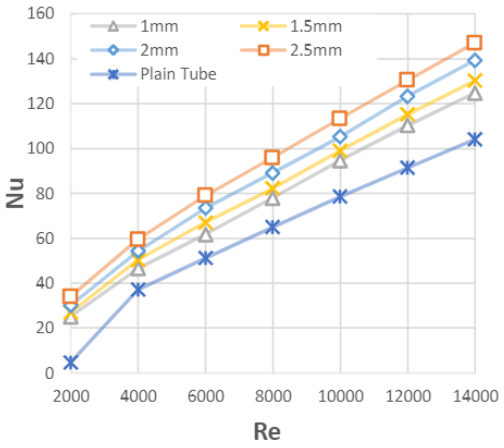

Figure 10. Variation of Nusselt number with Reynolds numbers at different dimple depths for pure water flows.

One can observe from Fig. 10 that both with increasing Reynolds number and the dimple depth, the Nusselt number increases. It is also seen in this figure that the increase in Nusselt number is more pronounced as flow regime changes from laminar regime (Re = 2000) to turbulent regime (Re=4000). This behavior is seen in both plain and dimpled tubes. In this transition region, it is seen that the rate of increase of the Nusselt number is higher in plain pipe flows than that of dimpled pipes. The reason for this phenomenon is that, for low Reynolds number flows, the presence of dimples in a tube surface affects the flow domain by generating vortices which disturb the flow and allow the flow to reach a turbulent state even at lower Reynolds numbers where the flow is considered to be laminar in a plain tube. (Suresh et al., 2011). In the fully turbulent flows, the increase in the Nusselt numbers is almost linear for both plain and dimpled pipes. Increasing the dimple depth also increases the tube surface area accordingly and in contrast, allow the convective heat transfer to occur far more efficiently, thereby increasing the Nusselt number (Firoozi, 2020).

In Fig. 11, variations of friction factor with Reynolds number in dimpled pipes with different dimple depths and plain pipe for pure water flow are given. In this figure it is clearly seen that dimples cause an increase in the friction factor compared to the plain tube as expected. In the transition region, as in the Nusselt number variation, the variation of the friction factor in plain pipe is also high compared to the dimpled tube flows. For the laminar flows, increase in the friction factor is much higher with increasing dimple depth.

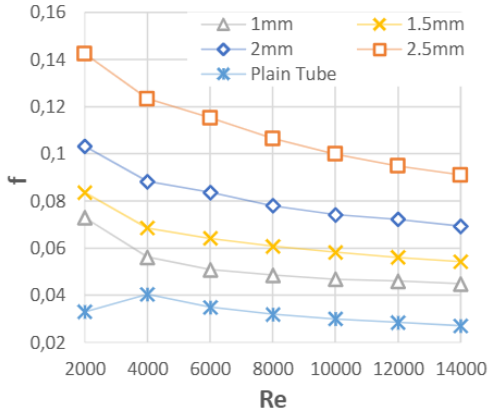

Figure 11. Variation of friction factor with Reynolds numbers at different dimple depths for water.

The performance evaluation criteria (PEC) which is an important tool to study the heat transfer and pressure drop within the capsule dimpled tubes calculated and plotted in Fig. 12. With the aid of PEC, performance of the dimpled tube can be evaluated considering both Nusselt number and friction factor effects.

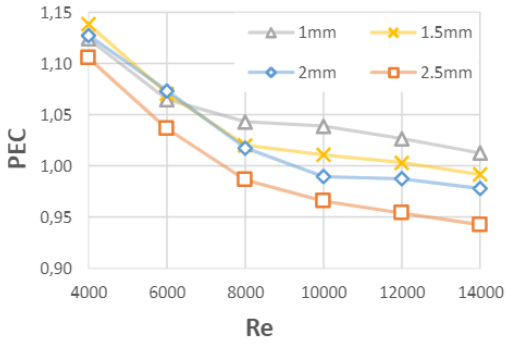

Figure 12. Variation of PEC with Reynolds numbers for different dimple depths for water.

As can be seen in Fig. 12, PEC values are decreasing with Reynolds number and dimple depth. For the transitional flow, (Re=4000-6000) 1.5 mm depth yields the best performance. However, as Re increases and flow becomes more and more turbulent, the dimples with 1 mm depth give better performance. It can be seen that, increasing dimple depth increases the performance till an optimum depth value. After that, especially in the turbulent region, PEC starts to drop. So when 2 mm dimple depth is used in the tubes, for the lower Reynolds Number flows (laminar and transition) it gives better performance, but when flow velocity increases and turbulence dominates, the friction factor does not fall, on the contrary it increases because of the dimples and performance decreases When the graphic is further examined, it can be seen that, 2.5 mm dimple depth has the worst characteristics since the friction factor

increases dramatically and flow becomes blocked due to decreased flow area for high dimple depths.

The effects of nanofluid

To investigate the effects of nanofluid on heat transfer enhancement, the simulations were performed for flows of Al_2O_3-water nanofluid with volumetric nanoparticle concentrations of 1%, 2% and 3% for different dimple depths (1.0, 1.5, 2.0 and 2.5 mm) and different Reynolds numbers. Again, from the simulated temperature, velocity, and pressure fields, Nusselt numbers, friction factors and performance evaluation criterion were calculated. For Nusselt number variation, it is noted that, increasing capsule depth increases Nusselt number more than the water flow in capsule dimpled pipes. In Fig. 13, PEC variation for 1% nanofluid is given as an example. Trends for all concentrations are similar.

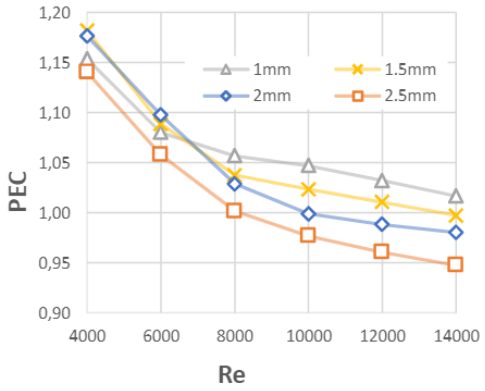

Figure 13. Variation of (PEC) with Reynolds numbers for different dimpled depths for Al_2O_3-water nanofluid with 1% concentration.

The variations of PEC with dimple depths at different Reynolds number and nano particle concentrations are shown in Fig. 14. As seen in these figures, at all lower Reynolds numbers (Re<8000) considered, PEC increases with increasing nano particle concentration. However, as Reynolds number increases, the effects of nano particles diminish.

In low Reynolds number flows, the presence of dimples affects the flow field by generating vortices which disturb the flow and allow the flow to reach a turbulent state even at lower Reynolds numbers where the flow is considered to be laminar in a plain tube. Hence, in the laminar region PEC increases with both increasing dimple depth and nanofluid concentration. This can be seen in Figure 14. PEC values for the laminar region are very high compared to transitional and turbulent flows.

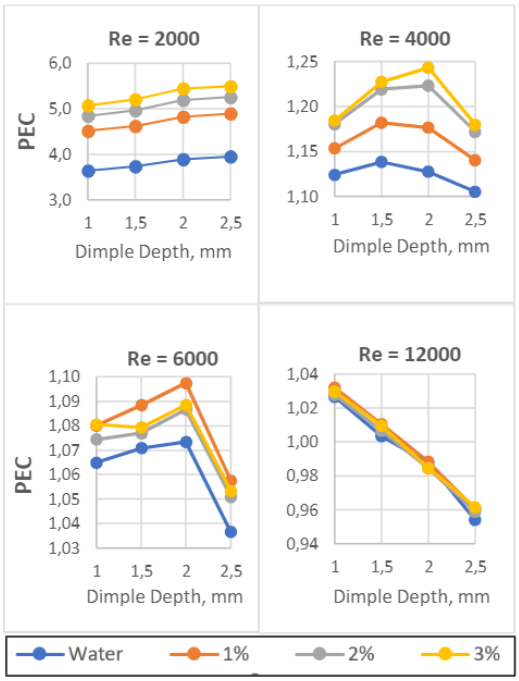

Figure 14. Effect of increasing dimple depth on PEC for different Reynolds Numbers for different nanofluid concentrations.

For the transition region, increase in volume concentration of nanofluid increases the PEC. On the other hand, as dimple depth increases, especially beyond 1.5 mm, it causes a reduction in performance for all cases. It should also be noted that with the increasing dimple depth, the blockage effects of the dimples increase which can cause and increase in friction coefficient. This may be because of the unpredictable flow phenomena that relates to the transition region.

On the early formation of turbulent flow around RE=6000, an increasing pattern in the PEC and a sudden drop can be seen around the 2 mm depth of dimple depth. In this region, 1 % in nanoparticle concentration of nanofluids shows best performance among all cases.

For a higher Re, (12000 for instance) The dimple depth adversely affects the performance since the friction factors are very high. The PECs drop dramatically with increasing depths. Moreover, the best performance is found for 1% nanofluid and a tube with a dimple depth of 1 mm.

CONCLUSION

A numerical investigation was carried out to investigate the heat transfer, pressure drop characteristics and performance evaluation criteria (PEC) for newly

proposed capsule dimpled tubes with pure water and Al_2O_3-water nanofluid as the working fluids. The study was performed for fully developed laminar, transition and turbulent flow conditions with uniform heat flux through the tube surface. The simulations were performed using ANSYS Fluent. For capsule dimpled tubes, three-dimensional; and for plain tubes, 2-D simulations were performed for steady state flow conditions.

Effects of Reynolds number, dimple depth, nano particle volumetric concentration on Nusselt number, friction factor and PEC were analyzed. The dimple depths varying between 1 and 2.5 mm, Reynolds numbers ranging between 2000-14000, nano particle concentration varying between 1% and 3% are considered in the numerical simulations.
The findings of the study can be summarized as following:

- For water as the heat transfer fluid, the Nusselt number increases with increasing dimple depths at all Reynolds numbers considered. Unfortunately, the friction factor also increases with increasing dimple depth. Hence, as PEC shows a significant increase in the laminar region, it starts to decrease gradually in the transition and then in the turbulent regions.
- For Al_2O_3-Water nanofluid as the heat transfer fluid, the trend of variation of Nusselt number, friction factor and PEC with Reynolds number is similar to those of pure water. Furthermore, for each dimple depth considered, as the nanoparticle concentration increases, Nusselt number and the friction factor increases significantly compared to plain tube.
- For small Re (laminar flow), higher depths of dimples seem to have a better performance due to the increase in Nusselt number for dimpled tube compared to plain tube.
- In high Reynolds numbers, the nanoparticle concentration has less effect on increasing PEC, since deeper dimples causes the friction factor to increase very much.
- A blockage phenomenon is observed when dimple depths become deeper. This acts as barrier against fluid flow, which in turn results in an increase in the friction factor and a decrease in PEC. This also depends on the Reynolds Number.

When considering PEC, the best performance among the cases studied are found as follows:

- For laminar region, 2.5 mm dimple depth and 3% nanoparticle concentration.
- For transition region, 2 mm dimple depth and 3% nanoparticle concentration.
- For early turbulence region (Re=6,000), 2 mm dimple depth and 1% nanoparticle concentration.
- For turbulence region (Re≥8,000), 1 mm dimple depth and 1% nanoparticle concentration.

REFERENCES

Alshehri, F., Goraniya, J., and Combrinck, M. L., 2020, Numerical investigation of heat transfer enhancement of a water/ethylene glycol mixture with Al_2O_3–TiO_2 nanoparticles. Applied Mathematics and Computation, 369, 124836.

Batchelor, G. K., 1977, The effect of Brownian motion on the bulk stress in a suspension of spherical particles. Journal of fluid mechanics, 83(1), 97-117.

Briclot, A., Henry, J. F., Popa, C., Nguyen, C. T. and Fohanno, S., 2020, Experimental investigation of the heat and fluid flow of an Al2O3-water nanofluid in the laminar-turbulent transition region. International Journal of Thermal Sciences, 158, 106546.

Cengel, Y., 2014, Heat and mass transfer: fundamentals and applications. McGraw-Hill Higher Education.

Chandrasekar, M., Suresh, S. and Bose, A. C., 2010, Experimental studies on heat transfer and friction factor characteristics of Al2O3/water nanofluid in a circular pipe under laminar flow with wire coil inserts. Experimental Thermal and Fluid Science, 34 (2), 122-130.

Cheraghi, M. H., Ameri, M. and Shahabadi, M., 2020, Numerical study on the heat transfer enhancement and pressure drop inside deep dimpled tubes. International Journal of Heat and Mass Transfer, 147, 118845.

Chen, J., Müller-Steinhagen, H. and Duffy, G. G., 2001, Heat transfer enhancement in dimpled tubes. Applied thermal engineering, 21 (5), 535-547.

Corcione, M., 2011, Empirical correlating equations for predicting the effective thermal conductivity and dynamic viscosity of nanofluids. Energy Conversion and Management, 52 (1), 789-793.

Eiamsa-Ard, S. and Promvonge, P., 2007, Heat transfer characteristics in a tube fitted with helical screw-tape with/without core-rod inserts. International Communications in Heat and Mass Transfer, 34 (2), 176-185.

Firoozi, A., Majidi, S. and Ameri, M., 2020, A numerical assessment on heat transfer and flow characteristics of nanofluid in tubes enhanced with a variety of dimple configurations. Thermal Science and Engineering Progress, 19, 100578.

Gee, D. L. and Webb, R. L., 1980, Forced convection heat transfer in helically rib-roughened tubes. International Journal of Heat and Mass Transfer, 23 (8), 1127-1136.

Ho, C. J., Chang, C. Y., Yan, W. M. and Amani, P., 2018, A combined numerical and experimental study on the forced convection of Al_2O_3-water nanofluid in a circular tube. International Journal of Heat and Mass Transfer, 120, 66-75.

Khedkar, R. S., Sonawane, S. S. and Wasewar, K. L., 2014, Heat transfer study on concentric tube heat exchanger using TiO2–water based nanofluid. International communications in Heat and Mass transfer, 57, 163-169.

Kukulka, D. J. and Smith, R., 2013, Thermal-hydraulic performance of Vipertex 1EHT enhanced heat transfer tubes. Applied Thermal Engineering, 61 (1), 60-66.

Kumar, A., Maithani, R. and Suri, A. R. S., 2017, Numerical and experimental investigation of enhancement of heat transfer in dimpled rib heat exchanger tube. Heat and Mass Transfer, 53 (12), 3501-3516.

Liu, B. Y. and Agarwal, J. K., 1974, Experimental observation of aerosol deposition in turbulent flow. Journal of Aerosol Science, 5 (2), 145-155.

Minea, A. A., 2017, Hybrid nanofluids based on Al2O3, TiO2 and SiO2: numerical evaluation of different approaches. International Journal of Heat and Mass Transfer, 104, 852-860.

Ming Li,Tariq S., Khana Ebrahim, Al-HajriaZahid and H.Ayubb, 2016, Single phase heat transfer and pressure drop analysis of a dimpled enhanced tube, Applied Thermal Engineering, 101, 2016, 38-46.

Maxwell, J. C., 1954, Electricity and magnetism (Vol. 2). New York: Dover.

Pak, B. C. and Cho, Y. I., 1998, Hydrodynamic and heat transfer study of dispersed fluids with submicron metallic oxide particles. Experimental Heat Transfer an International Journal, 11 (2), 151-170.

Pathipakka, G. and Sivashanmugam, P., 2010, Heat transfer behavior of nanofluids in a uniformly heated circular tube fitted with helical inserts in laminar flow. Superlattices and Microstructures, 47 (2), 349-360.

Sabir, R., Khan, M. M., Sheikh, N. A., Ahad, I. U. and Brabazon, D., 2020, Assessment of thermo-hydraulic performance of inward dimpled tubes with variation in angular orientations. Applied Thermal Engineering, 170, 115040.

Suresh, S., Chandrasekar, M. and Sekhar, S. C., 2011, Experimental studies on heat transfer and friction factor characteristics of CuO/water nanofluid under turbulent flow in a helically dimpled tube. Experimental Thermal and Fluid Science, 35(3), 542-549.

Tabatabaeikia, S., Mohammed, H. A., Nik-Ghazali, N. and Shahizare, B., 2014, Heat transfer enhancement by using different types of inserts. Advances in Mechanical Engineering, 6, 250354.

Vicente, P. G., García, A. and Viedma, A., 2002, Heat transfer and pressure drop for low Reynolds turbulent flow in helically dimpled tubes. International journal of heat and mass transfer, 45 (3), 543-553.

Wang, Y., He, Y. L., Lei, Y. G. and Zhang, J., 2010, Heat transfer and hydrodynamics analysis of a novel dimpled tube. Experimental thermal and fluid science, 34 (8), 1273-1281.

Xuan, Y. and Roetzel, W., 2000, Conceptions for heat transfer correlation of nanofluids. International Journal of heat and Mass transfer, 43 (19), 3701-3707.

Yimin X. and Qiang L., 2000, Heat transfer enhancement of nanofuids, International Journal of Heat and Fluid Flow, 21, 58-64.